

ToF-SIMS study of the surface morphology of blends of polystyrene and poly(*N*-vinyl-2-pyrrolidone) compatibilized by poly(styrene-co-4-vinylphenol)

X. M. Zeng,¹ L. T. Weng,² L. Li, C.-M. Chan,^{1*} S. Y. Liu¹ and M. Jiang³

¹ Department of Chemical Engineering, Biotechnology Research Institute, Hong Kong University of Science & Technology, Clear Water Bay, Kowloon, Hong Kong

² Materials Characterization and Preparation Facility, Hong Kong University of Science & Technology, Clear Water Bay, Kowloon, Hong Kong

³ Institute of Macromolecule Science and Laboratory of Molecular Engineering of Polymers, Fudan University, Shanghai 200433, P. R. China

Received 5 September 2000; Revised 5 February 2001; Accepted 8 February 2001

The influence of the vinylphenol content of poly(styrene-co-4-vinylphenol) (STVPh) on the surface morphology of a blend of polystyrene (PS) and poly(*N*-vinyl-2-pyrrolidone) (PVP) was investigated by time-of-flight secondary ion mass spectrometry (ToF-SIMS) chemical imaging. The images obtained through the use of the ToF-SIMS positive total ions and selected negative ions clearly show that the characteristic size of the dispersed phase (PVP) decreased with the addition of the STVPh-5 (5 mol.% vinylphenol) random copolymer. The spectra obtained retrospectively from the matrix and the dispersed phase indicated that the matrix phase was very similar to the pure PS and that the dispersed phase was very similar to the pure PVP. The addition of the STVPh-9 random copolymer to the blend of PS and PVP resulted in a totally different morphology: both PVP and PS became semi-continuous and the dispersed particles are much larger. The morphological changes were caused by the formation of a single phase between PVP and STVPh-9 due to an increase in the density of the hydrogen bond formed between PVP and STVPh-9. When the vinylphenol content was <2 mol.%, the particle size of the PVP-rich phase stayed the same. The compatibilizing effect was much weakened as the concentration of STVPh-5 decreased to 1 wt.%. Copyright © 2001 John Wiley & Sons, Ltd.

KEYWORDS: ToF-SIMS; polymers; blend; polystyrene; morphology

INTRODUCTION

Blending immiscible polymers could be an effective method for obtaining the required properties of the final materials. The properties of an immiscible polymer blend depend highly on the interfacial adhesion between the phases. However, simple mixing of two or more polymers would result only in poor adhesion between them. In order to overcome this problem, a compatibilizer^{1–5} usually is added to an immiscible blend to increase its interfacial adhesion. Through the use of a compatibilizer, the morphology of an immiscible polymer blend is changed.

Block or graft copolymers have been used widely as compatibilizers.^{6–14} Nevertheless, only a few block copolymers that are produced by anionic polymerization are available.¹⁵ In addition, the long block copolymer molecules prefer to form micelles than to migrate to the

interface.^{16,17} In practice, random copolymers could be good compatibilizers that are relatively easy to synthesize at low cost. Recently, Dai *et al.* investigated the immiscible blend of polystyrene (PS) and poly(2-vinylpyridine) (PVPy) compatibilized by a random copolymer of deuterated PS and PVPy⁵ and a random copolymer of poly(styrene-co-2-vinylpyridine) (STVPh).¹⁸ They found that the long, random copolymers could be remarkably effective in reinforcing the immiscible polymer blend interfaces. The strengthening of the interface of the blend of PS and poly(methyl methacrylate) (PMMA) by a random copolymer of PS and PMMA was studied by Kulasekera *et al.*¹⁹ A recent study²⁰ was undertaken on the fracture toughness of the PS/PMMA immiscible blend compatibilized by three different kinds of copolymer–diblock, graft and random copolymers. The results indicated that the diblock copolymer was more effective as a coupling agent in this system. However, an even more recent study²¹ that compared polystyrene/poly(2-vinylpyridine) graft, block and random copolymers suggested that the use of block or graft copolymers may not be necessary in cases where strengthening is realized through the formation of hydrogen bonds. Fundamental experiments on the role of the copolymer at the interface and, in particular, its effect on the surface behaviour have become an intensive research

*Correspondence to: C.-M. Chan, Department of Chemical Engineering, Biotechnology Research Institute, Hong Kong University of Science & Technology, Clear Water Bay, Kowloon, Hong Kong.
Contract/grant sponsor: Hong Kong Government Research Grants Council; Contract/grant number: HKUST 9123/97P.
Contract/grant sponsor: Biotechnology Research Institute; Contract/grant number: TCMRPS/5/97.

area, but the mechanism responsible for the compatibilizing effect in many immiscible blend systems is still not fully established.

The compatibilizing effect of random, block or graft copolymers on immiscible polymer blends is important to many industrial applications. However, most studies focused on melt-mixing immiscible blends, because melt-mixing is the most common method of preparing mixtures. Recently, thin polymer films prepared by spin-coating have attracted significant interest because the surface properties of these films, e.g. wettability, adhesion, biocompatibility and coefficient of friction, have been identified as the critical parameters for many advanced technological applications. Thin polymer films are used in many industrial applications, such as photonic bandgap materials²² and photoresist layers of integrated circuits.²³ If the polymers are immiscible, demixing takes place during the solution-casting process.²⁴ Different domain morphologies that form during the solvent evaporation process are observed. In general, the surface morphology of polymer blends has been characterized mainly by using scanning electron microscopy (SEM), optical microscopy and atomic force microscopy (AFM). However, an important problem in the study of morphology of the compatibilizing blends is that the chemical nature of the compatibilizer may be partially identical or similar to the components of the blend. Therefore, it is very difficult to identify the compatibilizer from the rest of the sample and then to tell whether it is located at the interface or in one phase of the blend. Recently, a time-of-flight secondary ion mass spectrometry (ToF-SIMS) chemical imaging technique has been developed. It is an effective method for the characterization of polymer surfaces, providing information on elemental composition, molecular structure²⁵ and surface morphology.^{26–30} For example, this technique was used successfully to examine the morphology and miscibility of ethylene–tetrafluoroethylene copolymer and PMMA blends.³⁰

The purpose of this study is to investigate the compatibilizing effect of the poly(styrene-co-4-vinylphenol) random copolymer on an immiscible PS and poly(*N*-vinyl-2-pyrrolidone) (PVP) blend by using ToF-SIMS chemical imaging. Three random copolymers of STVPh with 2, 5 and 9 mol.% of vinylphenol (STVPh-2, STVPh-5 and STVPh-9) were used as compatibilizers. The effect of the concentration of STVPh-5 on the surface morphology of the PS/PVP/STVPh-5 blend also was investigated.

EXPERIMENTAL

Materials

The homopolymers used in this investigation were PS and PVP. The PS was purchased from Aldrich Chemical Co. and PVP was obtained from Sigma Chemical Inc. The random copolymers (STVPh-2, STVPh-5 and STVPh-9, containing 2, 5 and 9 mol.% vinylphenol, respectively) were synthesized via a demethylation reaction.³¹ The molar contents of vinylphenol in STVPh were obtained from ¹H-NMR measurement.³¹ Glass transition temperature measurements were carried out with a TA 2910 differential scanning calorimeter at a heating

rate of 10 °C min⁻¹ from zero to 220 °C. Differential scanning calorimeter (DSC) traces were recorded in the second heating cycle. The vinylphenol contents, molecular weights, polydispersity and glass transition temperatures of PS, PVP and the random copolymers are shown in Table 1.

Sample preparation

The STVPh random copolymers were dissolved in tetrahydrofuran (THF). Both PS and PVP were dissolved in a mixture of THF and methanol at a concentration of 6 g l⁻¹. The compatibilized samples were prepared by mixing the solution of the random copolymer and the solution of PVP and PS. Dimethyl formamide (DMF) was added to the solution of the PS/PVP/STVPh-9 blend to prevent precipitation. Films of the PS/PVP, PS/PVP/STVPh-2 and PS/PVP/STVPh-5 blends were obtained by spin-casting the polymer blend solutions onto silicon wafers. The film of the blend of PS/PVP/STVPh-9 was prepared by solution-casting in a vacuum oven. Cast films then were dried in a vacuum at room temperature in order to remove the residue solvent.

Surface morphology characterization

Surface characterization was performed on a PHI 7200 ToF-SIMS spectrometer.^{28,30} The surface chemical images of the PS and PVP blends were acquired in both positive and negative ion modes by the use of a Ga⁺ beam at 25 keV. In order to obtain high spatial resolution images, an ion pulse width of ~50 ns was used. The total ion dose for each image acquisition was <4 × 10¹¹ ions cm⁻². The charge compensation was realized with a pulsed low-energy (0–70 eV) flooding gun. The data in this work were acquired in 'raw-data-stream' mode.^{28,30} In this mode, any image from a selected peak (or a group of peaks) or any mass spectrum from a selected imaged area can be created retrospectively. Both positive and negative high-mass-resolution spectra of pure PS, PVP and STVPh samples were obtained by using a 15 keV Ga⁺ ion source.

RESULTS AND DISCUSSION

Typical ToF-SIMS positive spectra of the pure PS and PVP film surfaces are shown in Fig. 1. These spectra were obtained by using a 15 keV Ga⁺ ion gun (mass resolution ~5000). Both PS and PVP spectra are consistent with previous data.^{32,33} The positive spectrum of PS is characterized by a series of aromatic ions at *m/z* = 77 (C₆H₅⁺), 91 (C₇H₇⁺), 103 (C₈H₇⁺), 105 (C₈H₉⁺) and 115 (C₉H₇⁺). The spectrum of

Table 1. Characteristics of homopolymers and random copolymers

Polymer	VPh content (mol.%)	$M_n \times 10^{-3}$ (g mol ⁻¹)	M_w/M_n	T_g (°C)
PS		200		105.2
PVP		360		178.8
STVPh-2	2.86	89.5	1.60	106.1
STVPh-5	5.20	121.7	1.28	108.6
STVPh-9	9.02	101.8	1.52	111.9

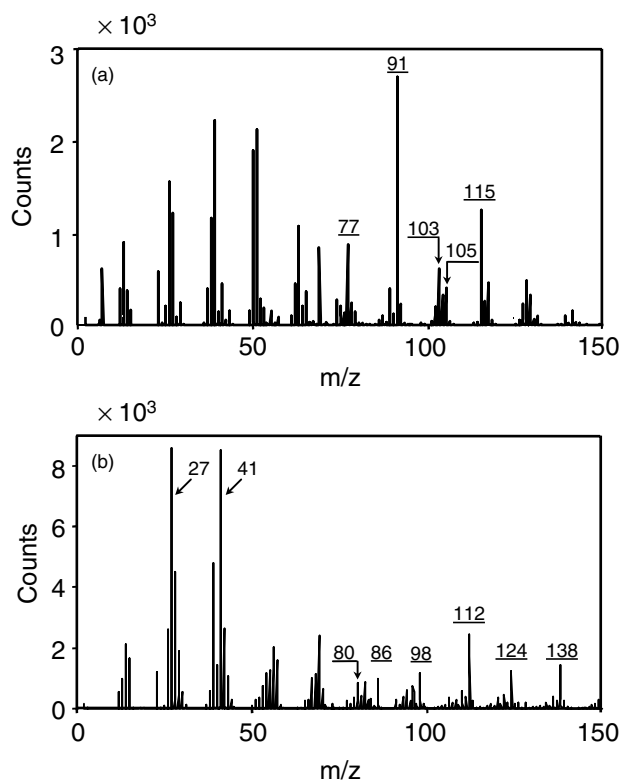
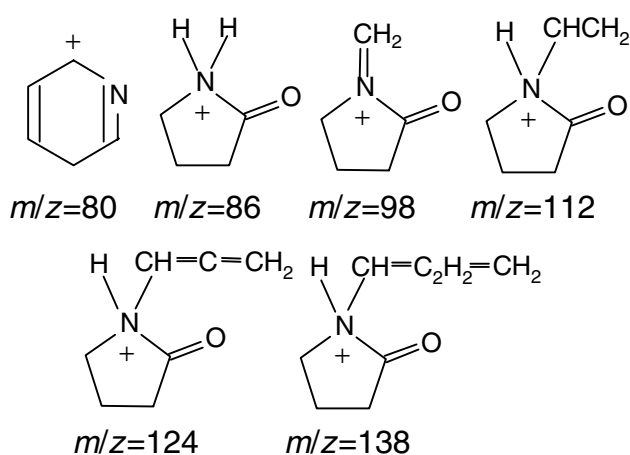


Figure 1. The positive ion spectra of pure PS (a) and pure PVP (b).

PVP is distinguished from that of PS by the presence of a series of characteristic nitrogen-containing peaks at $m/z = 80$ ($C_5H_6N^+$), 86 ($C_4H_8NO^+$), 98 ($C_5H_8NO^+$), 112 ($C_6H_{10}NO^+$), 124 ($C_7H_{10}NO^+$) and 138 ($C_8H_{12}NO^+$). The peaks at $m/z = 27$ ($C_2H_3^+$) and 41 ($C_3H_5^+$) are the common intense peaks for both polymers. The proposed structures of some of the positive characteristic ions for PVP are shown below:¹⁴



The negative ion spectra of pure PS and PVP are shown in Fig. 2. The negative spectrum of PS is dominated by hydrocarbon peaks at $m/z = 13$ (CH^-), 25 (C_2H^-), 37 (C_3H^-), 49 (C_4H^-), 62 ($C_5H_2^-$) and 73 (C_6H^-). The negative ion spectrum of PVP is distinguished from that of PS by the appearance of the characteristic peaks at $m/z = 16$ (O^-), 17 (OH^-), 26 (CN^-), 42 (CNO^-) and 84 ($C_4H_6NO^-$). However,

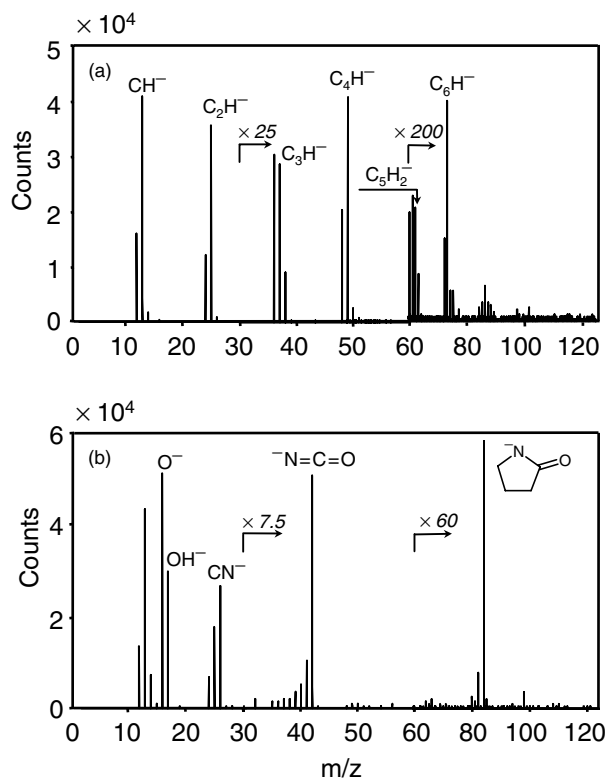


Figure 2. The negative ion spectra of pure PS (a) and pure PVP (b).

the peak intensity of PVP at $m/z = 25$, 37, 49, 62 and 73 is relatively low. Therefore, it is, in principle, possible to use the peaks at $m/z = 16$, 17, 26, 42 and 84 to map PVP and the peaks at $m/z = 25$, 37, 49, 62 and 73 to map PS. The surface morphological changes of the PVP and PS blends were investigated by ToF-SIMS chemical imaging using the positive total ions and the selected characteristic negative ions of PVP, i.e. ($O^- + OH^-$) and CN^- . Ions CNO^- and $C_4H_6NO^-$ were not used because their intensities are very low. On the contrary, the more intense negative ion, C_2H^- ($m/z = 25$), could be selected for imaging, even though it is not a unique peak of PS, because the intensity of the peak is much higher in the PS spectrum than in the PVP spectrum. The image constructed from C_2H^- of PS should be complementary to those constructed from ($O^- + OH^-$) and CN^- of PVP.

Figure 3(a) shows the ToF-SIMS chemical images of the PS/PVP blend (70/30 weight ratio) obtained through the use of positive total ions. The image shows that phase separation occurred during film formation. Because the secondary ion yield is higher for PVP than for PS, the PVP-rich phase appears brighter than the PS-rich phase. The positive spectra (not shown) obtained retrospectively from the continuous PS-rich phase (phase A) and the dispersed PVP-rich phase (phase B), as shown in Fig. 3(a), are almost identical to those of pure PS and PVP (Fig. 1). These results indicate that phase separation occurs on the surface of the PS/PVP immiscible blend.

The negative ion images of the PS/PVP (70/30 weight ratio) blend, as shown in Figs 3(b) and 3(c), were obtained using the characteristic PVP negative ions ($O^- + OH^-$) and

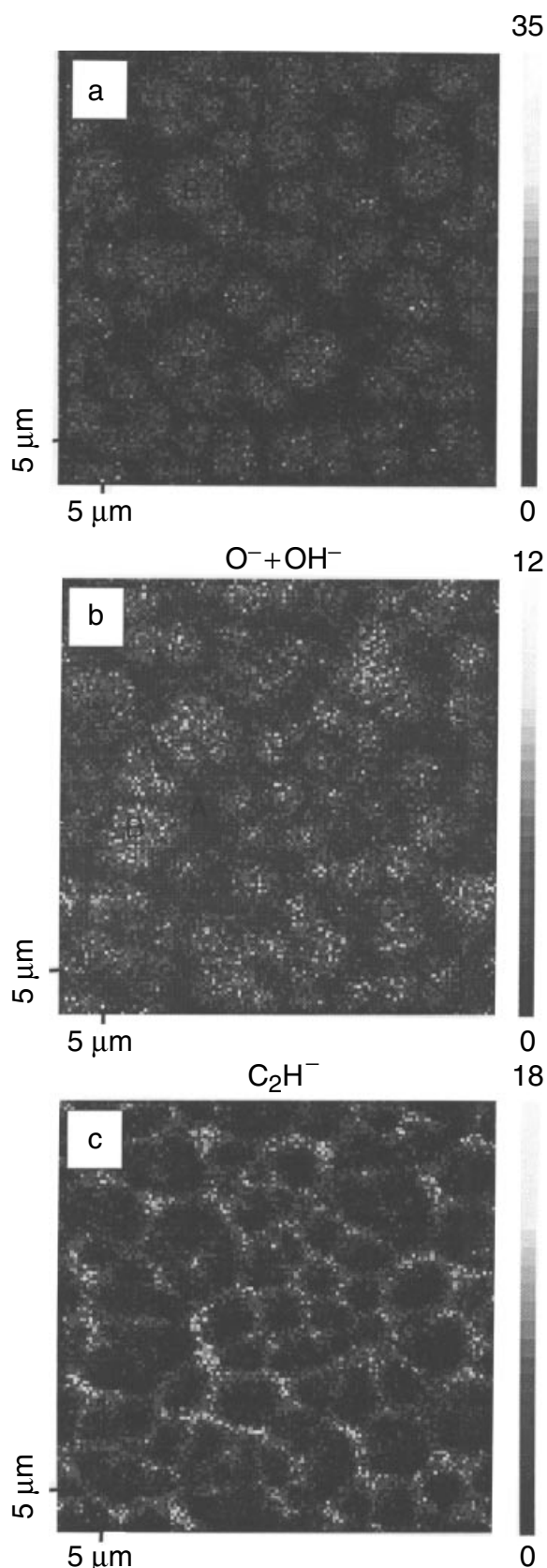


Figure 3. The ToF-SIMS images of the PS/PVP (70/30) blend obtained using the positive total ion (a), $O^- + OH^-$ (b) and C_2H^- (c).

the intense PS negative ion C_2H^- . The light areas in Fig. 3(b) represent the PVP-rich phase and the dark areas reveal the

PS-rich phase. On the contrary, light areas in Fig. 3(c) correspond to the PS-rich phase. Obviously, the images obtained from $(O^- + OH^-)$ and C_2H^- are highly complementary. The negative spectra obtained retrospectively from the continuous PS-rich phase (phase A) and the dispersed PVP-rich phase (phase B) are very similar to those obtained with pure PS and PVP, as shown in Fig. 2.

The morphology of the PS/PVP/STVPh-2 (65/30/5 weight ratio) blend was performed by the ToF-SIMS study. The particle sizes are very similar to those of the PS/PVP blend, indicating no reduction in particle size. This may be explained by the low vinylphenol content in the copolymer.

Figure 4 shows the positive total ion images and the negative ion images of the PS/PVP/STVPh-5 (65/30/5 weight ratio) blend obtained through the use of total positive ion, $(O^- + OH^-)$ and C_2H^- . A comparison between Figs 3 and 4 shows that the characteristic size of the PVP dispersed phase decreases dramatically when the random copolymer (STVPh-5) is added to the blend as a compatibilizer. The average diameter of the dispersed PVP particles is $\sim 2\text{--}3\ \mu\text{m}$ in the PS/PVP/STVPh-5 blend, which is several times smaller than the size of the PVP particles ($\sim 7\ \mu\text{m}$) in the PS/PVP blend. The presence of a suitable random copolymer at the interface lowers the interfacial tension between the immiscible phases of a blend.⁸ A lower interfacial tension produces particles of smaller sizes in the dispersed phase. Although the interfacial layer of STVPh-5 cannot be observed in the ToF-SIMS chemical image, it is logical to conclude that the reduction in the PVP particle size is a result of migration of the STVPh-5 random copolymer to the interface between the PS and PVP phases.

The formation of hydrogen bonds between the carbonyl and hydroxyl groups has been studied previously.^{34,35} In our study, hydrogen bonds are expected to be formed between STVPh-5 and PVP. The compatibilizing effect in the blends of PS and PVP is due to the fact that the affinity between the PS homopolymer and the PS blocks of STVPh-5 is balanced by the interaction between the carbonyl groups of PVP and the hydroxyl groups of STVPh-5. This leads to the localization of STVPh-5 at the interface between PS and PVP. Furthermore, the balanced interaction is likely to influence the morphology of the PS and PVP blend.

The negative ion images of the PS/PVP/STVPh-9 (65/30/5 weight ratio) blend are shown in Fig. 5. These images were obtained using $(O^- + OH^-)$ and CN^- of PVP and the intense C_2H^- ion of PS. The image obtained from the selected ion peaks of $O^- + OH^-$ looks brighter than the CN^- image because the intensity of CN^- is lower. Figure 5 shows that both the PVP-rich and the PS-rich phases become semi-continuous, i.e. that in some areas the PVP-rich phase is the dispersed phase (upper part of the images), whereas in the other areas the PS-rich phase is the dispersed phase (lower part of the images). Unlike the PS/PVP and the PS/PVP/STVPh-5 blends, much larger dispersed particles are seen, indicating a decrease in the compatibility between PS and PVP. Although PS, PVP and STVPh-9 are individually soluble in the mixture of THF and methanol, the PS/PVP/STVPh-9 blend is not soluble in this mixture. However, the blend becomes soluble after the

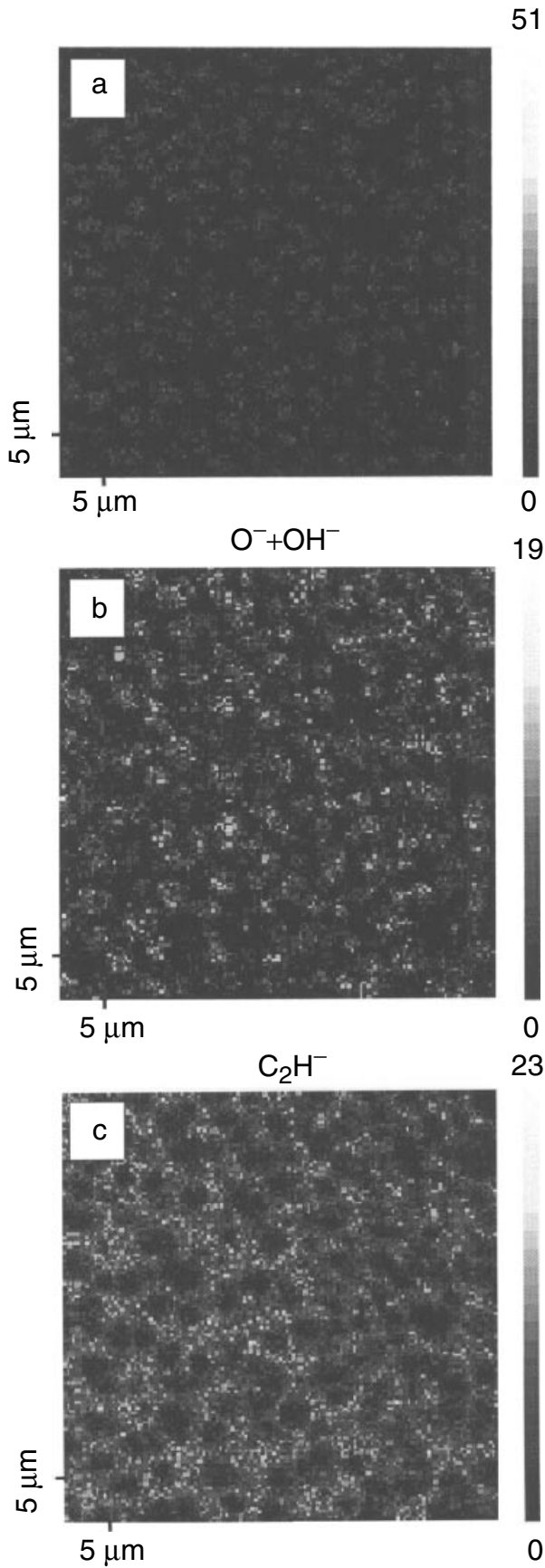


Figure 4. The ToF-SIMS images of the PS/PVP/STVPh-5 (65/30/5) blend obtained using the positive total ion (a), $O^- + OH^-$ (b) and C_2H^- (c).

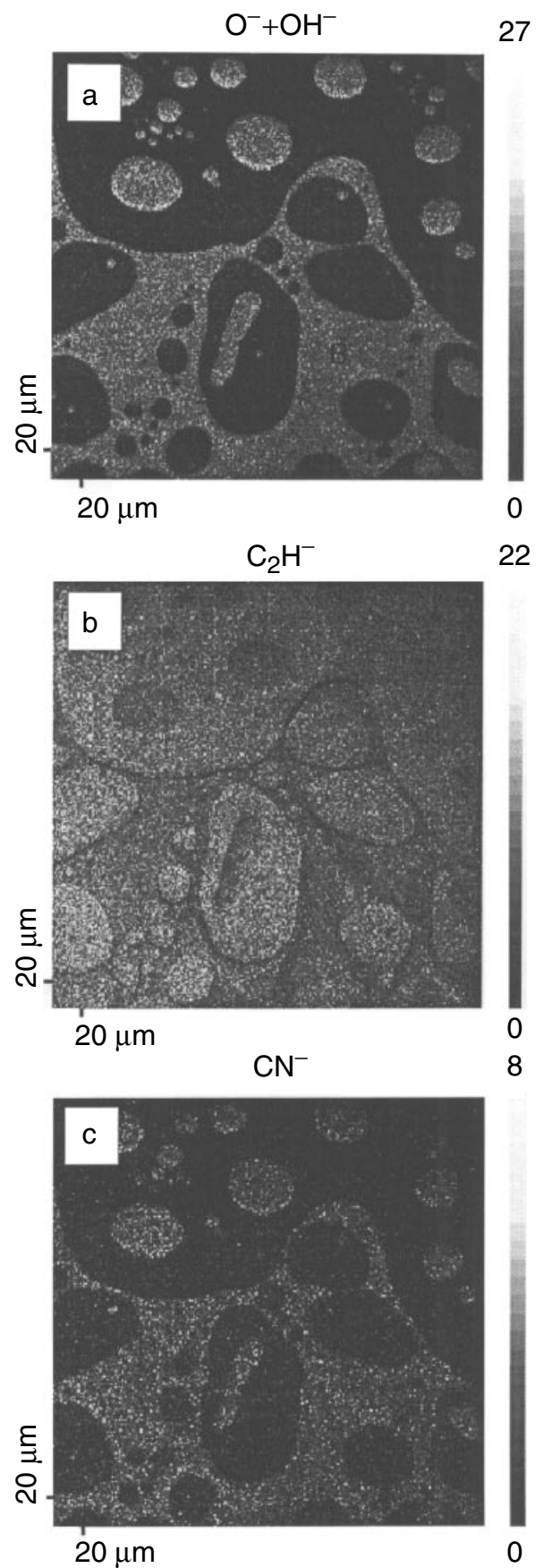
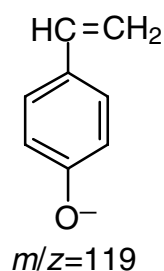


Figure 5. The ToF-SIMS images of the PS/PVP/STVPh-9 (65/30/5) blend obtained using $O^- + OH^-$ (a), C_2H^- (b) and CN^- (c).

addition of a small amount of DMF. When the concentration of the hydroxyl groups in STVPh increases, the density of the hydrogen bond formed between PVP and STVPh-9 increases. The increase in the density of the hydrogen bond is the cause for precipitation of the PS/PVP/STVPh-9 blend in the mixture of THF and methanol, indicating that a complex with strong intermolecular interaction is formed at a high vinylphenol content.

The negative spectra of STVPh-9 and spectra obtained retrospectively from the PS-rich phase (phase A) and the PVP-rich phase (phase B) as shown in Fig. 6 strongly indicate that STVPh-9 is dispersed in the PVP-rich phase. This is demonstrated in Fig. 6(c) by the presence of a most characteristic negative peak of STVPh at $m/z = 119$. This ion comes from the vinylphenol part of the main chain of STVPh [cf. Fig. 6(a)]. The structure of this ion is shown below:



This is supported also by the observation of the higher intensities of the peaks at $m/z = 25$ (C_2H^-), 49 (C_4H^-) and 73 (C_6H^-) in the PVP-rich phase than in pure PVP [Fig. 2(b)]. As explained above, these ions are more intense in PS [Fig. 2(a)] and STVPh [Fig. 6(a)]. Because PS and PVP are not miscible, these peaks in the PVP-rich phase are mainly due to STVPh-9. The contribution of C_2H^- of STVPh-9 in the PVP-rich phase also results in the reduction in the contrast of the C_2H^- image, as shown in Fig. 5(b), which is not as good as those shown in Figs 3(c) and 4(c).

The distribution of STVPh-9 in the PS/PVP/STVPh-9 blend can be obtained also from a detailed analysis of the positive spectra. Figure 7 shows the positive SIMS spectra of pure STVPh-9 and the spectra obtained retrospectively from the PS-rich and PVP-rich phases of PS/PVP/STVPh-9 (65/30/5). The aromatic peaks at $m/z = 77$ ($C_6H_5^+$) and 91 ($C_7H_7^+$) are characteristic of PS [Fig. 1(a)] and STVPh.³⁴ In the PVP spectrum [Fig. 1(b)], the intensity of these peaks is very low. However, the intensity of these peaks is much higher in the spectrum of the PVP-rich phase, as shown in Fig. 7(c). Because PS and PVP are immiscible, the presence of these peaks is a strong indication that STVPh-9 is present in the PVP-rich phase. This is consistent with the analysis of negative ion spectra. Another characteristic positive ion of STVPh is $C_7H_7O^+$ at $m/z = 107$.³⁶ The peak at $m/z = 107$ is very small in the spectra of pure PVP [Fig. 1(b)] and the PS-rich phase (Fig. 7b). However, the intensity of this peak in the spectrum of the PVP-rich phase [Fig. 7(c)] is relatively high, indicating the presence of STVPh-9. It should be noted here that the intensity of peak at $m/z = 107$, as shown in Fig. 7(c), is not as strong as that in the pure STVPh-9. This can be explained by the lower concentration of STVPh-9 in the blend.

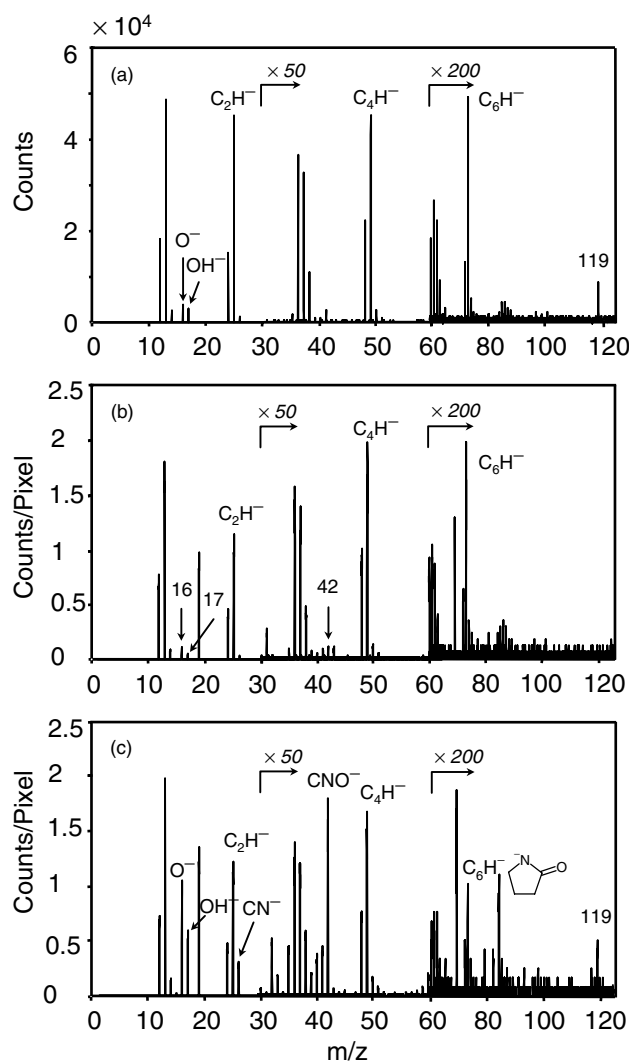


Figure 6. Negative SIMS spectra of pure STVPh-9 (a), the PS-rich phase in the PS/PVP/STVPh-9 (65/30/5) blend (b) and the PVP-rich phase in the PS/PVP/STVPh-9 (65/30/5) blend (c).

The above results indicate that when the VPh content increases beyond 9 mol.%, PVP and STVPh-9 become miscible. Similarly, the result of a study of the blends of STVPh (VPh content 1–100 mol.%) and poly(styrene-co-4-vinylpyridine) (vinylpyridine content was 72 mol.%) indicated that the miscibility of STVPh and poly(styrene-co-4-vinylpyridine) increased when the VPh content increased.³⁶ Therefore, it can be concluded that the PS/PVP/STVPh-9 blend is an immiscible blend of PS and a miscible blend of PVP and STVPh-9. These results show that STVPh-9 cannot be used as a compatibilizer for the blend of PS and PVP. On the other hand, the random copolymer (STVPh-5) is a good compatibilizer because the interaction between PVP and STVPh-5 is balanced by the affinity of PS and the PS blocks of the STVPh-5, leading to the localization of STVPh-5 at the interface between the PS and PVP phases.

The phase continuity and inversion in polymer blends have been shown to be related to the volume fraction and viscosity of the components.^{37,38} In the PS/PVP/STVPh-5 (65/30/5) blend the ratio of the PS volume fraction to the PVP volume fraction was ~ 2.2 . Whereas in the PS/PVP/STVPh-9

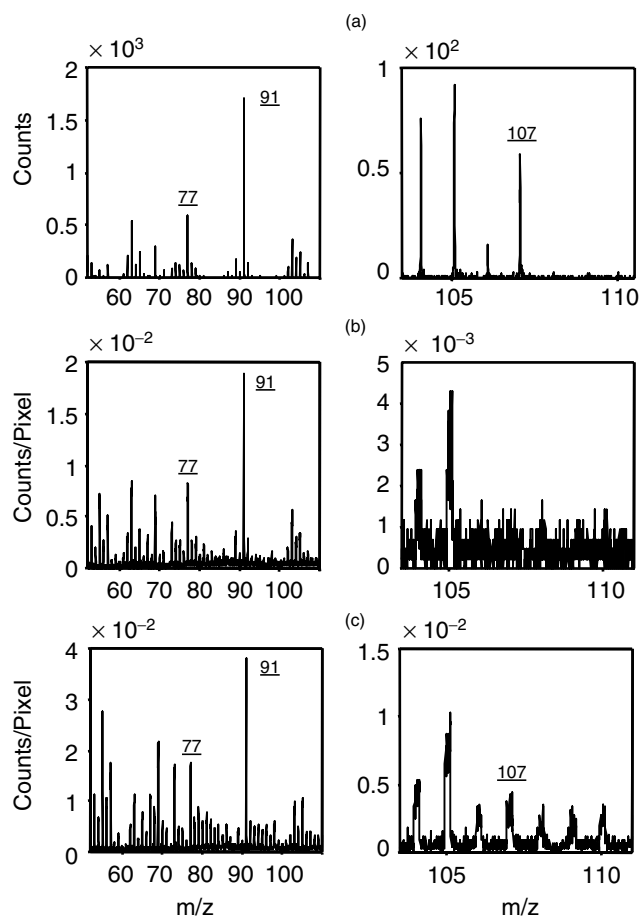


Figure 7. Positive SIMS spectra of pure STVPh-9 (a), the PS-rich phase of the PS/PVP/STVPh-9 blend (b) and the PVP-rich phase of the PS/PVP/STVPh-9 blend (c).

(65/30/5) blend the ratio of the PS volume fraction to the PVP/STVPh-9 volume fraction was close to 1.9. The change in the ratio of the volume fraction and viscosity of the components could be the driving force for the observed differences in the surface morphology of these three blend systems. In addition, it is known that the solvents can have significant effects on the morphology of the blends and the polymer–polymer interactions.³⁹ In this work, the effects of solvents on the morphology have not been studied.

The optical micrographs showing the morphology of the PS/PVP/STVPh-5 blend with different concentrations of STVPh-5 are shown in Fig. 8. At a low STVPh-5 concentration (<1 wt.%), the size of the PVP stays relatively constant. As the concentration increases to >3 wt.%, a significant decrease in the particle size of the PVP dispersed phase is observed, as shown in Figs 8(c) and 8(d). These results show that the concentration of the compatibilizer has a significant effect on the particle size of the dispersed phase.

The surface morphology of the PS/PVP/STVPh-9 blend was studied also by optical microscopy. The optical micrograph shows a similar morphology to that revealed by the SIMS images. However, from the optical micrograph it is impossible to determine the chemical nature of the phases. Therefore, the ToF-SIMS chemical imaging technique is a powerful tool for studying the surface properties and morphology of immiscible polymer blends.

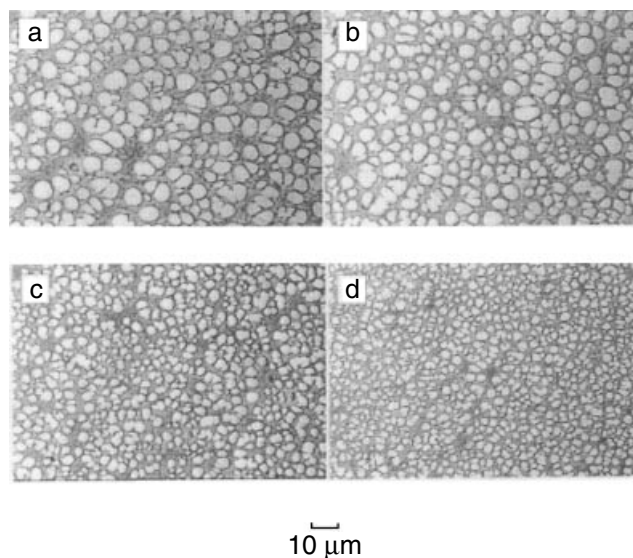


Figure 8. Optical micrographs of the PS/PVP blend (a) and the PS/PVP/STVPh-5 blends with STVPh-5 at concentrations of 1 wt.% (b), 3 wt.% (c) and 5 wt.% (d).

CONCLUSION

The effect of the random copolymer STVPh on the compatibility of PS and PVP immiscible blends was investigated. The addition of STVPh-5 to the blend results in a significant decrease in the characteristic size of the PVP dispersed phase, as revealed by ToF-SIMS chemical imaging. The change in the dispersed phase morphology is believed to be caused by the migration of the STVPh-5 random copolymer to the interface between the PS and PVP phases. The addition of another random copolymer, STVPh-9, produced a totally different morphology: PVP and PS became semi-continuous. The PS/PVP/STVPh-9 is an immiscible blend of PS and a miscible blend of PVP and STVPh-9. At low STVPh-5 concentrations, the size of the dispersed PVP phase stayed relatively constant. When the concentration increases to 3 wt.%, a significant reduction in the size of the dispersed phase was observed. These results have shown that ToF-SIMS chemical imaging is a very effective technique for studying the surface properties and morphology of polymer blends.

Acknowledgements

This work was supported by the Hong Kong Government Research Grants Council under grant no. HKUST 9123/97P and the Biotechnology Research Institute under grant no. TCMRPS/5/97.

REFERENCES

1. Brown HR, Deline VR, Green PF. *Nature* 1989; **341**: 221.
2. Creton CF, Kramer EJ, Hui C-Y, Brown HR. *Macromolecules* 1992; **25**: 3075.
3. Winey KI, Berba ML, Galvin ME. *Macromolecules* 1996; **29**: 2868.
4. Lee MS, Lodge TP, Macosko CW. *J. Polym. Sci. Part B: Phys.* 1997; **35**: 2835.
5. Dai C-A, Osuji CO, Jandt KD, Dair BJ, Ober CK, Kramer EJ, Hui C-Y. *Macromolecules* 1997; **30**: 6727.
6. Helfand E. *Macromolecules* 1975; **8**: 552.
7. Noolandi J, Hong KM. *Macromolecules* 1984; **17**: 1531.
8. Ouhadi T, Fayt R, Jerome R, Teyssie Ph. *J. Appl. Polym. Sci.* 1986; **32**: 5647.

9. Dai KH, Kramer EJ. *Polymer* 1994; **35**: 157.
10. Brown HR, Char K, Deline VR, Green PF. *Macromolecules* 1993; **26**: 4155.
11. Char K, Brown HR, Deline VR. *Macromolecules* 1993; **26**: 4164.
12. Zhao H, Huang B. *J. Appl. Polym. Sci.* 1998; **36**: 85.
13. Dai C-A, Jandt KD, Iyengar DR, Slack NL, Dai KH, Davidson WB, Kramer EJ, Hui C-Y. *Macromolecules* 1997; **30**: 549.
14. Feng H, Ye HC, Tian J, Feng Z, Huang B. *Polymer* 1998; **39**: 1787.
15. Genzer J, Composto RJ. *Macromolecules* 1998; **31**: 870.
16. Leibler L. *Macromol. Chem., Macromol. Symp.* 1988; **16**: 1.
17. Xu Z, Kramer EJ, Edgcombe BD, Fréchet MJ. *Macromolecules* 1997; **30**: 7958.
18. Dai CA, Dair BJ, Dai KH, Kramer EJ, Hui C, Jelinski LW. *Phys. Rev. Lett.* 1994; **73**: 2472.
19. Kulasekera H, Kaiser H, Ankner JF, Russell TP, Brown HR, Hawker CJ, Mayes AM. *Macromolecules* 1996; **29**: 5493.
20. Cho K, Ahn TO, Ryu HS, Seo KH. *Polym. Commun.* 1996; **37**: 4849.
21. Brian DE, Stein JA, Fréchet MJ, Xu Z, Kramer EJ. *Macromolecules* 1998; **31**: 1292.
22. Haus JW. In *Quantum Optical Confined Systems*, Ducloy M, Block D (eds). Kluwer Academic: Dordrecht, 1996.
23. Service RF. *Science* 1997; **278**: 383.
24. Böltau M, Walheim S, Mlynek J, Krausch G, Steiner U. *Nature* 1998; **391**: 877.
25. Feast WJ, Munro HS, Richards RW. *Polymer Surfaces, Interfaces II*. John Wiley: Chichester, 1993; 221.
26. Briggs D, In Feast WJ, Munro HS (eds). *Polymer Surface and Interfaces*, John Wiley: Chichester, 1987; 33.
27. Brown A, Vickerman JC. *Analyst* 1984; **109**: 851.
28. Reichlmaier S, Bryan SR, Briggs D. *J. Vac. Sci. Technol. A* 1995; **13**: 1217.
29. Briggs D, Fletcher IW, Reichlmaier S, Agulo-Sanchez JL, Short RD. *Surf. Interface Anal.* 1996; **24**: 419.
30. Weng LT, Smith TL, Feng J, Chan C-M. *Macromolecules* 1998; **31**: 929.
31. Xiang ML, Jiang M, Feng L. *Macromol. Rapid Commun.* 1995; **16**: 477.
32. Briggs D, Brown A, Vickerman JC, *Handbook of Static Secondary Ion Mass Spectrometry*, John Wiley: Chichester, 1989.
33. Weng LT, Bertrand P, Lauer W, Zimmer R, Busetti S. *Surf. Interface Anal.* 1995; **23**: 879.
34. Li L, Chan C-M, Weng LT. *Polymer* 1998; **39**: 2355.
35. Zhu KJ, Chen SF, Ho Tai, Pearce Eli M, Kwei TK. *Macromolecules* 1990; **23**: 150.
36. Li L, Chan C-M, Weng LT, Xiang M-L, Jiang M. *Macromolecules* 1998; **31**: 7248.
37. Jordhamo GM, Manson JA, Sperling LH. *Polym. Eng. Sci.* 1986; **26**: 517.
38. Zhu S-H, Chan C-M. *Polymer* 1998; **39**: 7023.
39. Zeng X-M, Chan C-M, Weng L-T, Li L. *Polymer* 2000; **41**: 8321.